

Scotland's Rural College

Stereological assessment of sexual dimorphism in the rat liver reveals differences in hepatocytes and Kupffer cells but not hepatic stellate cells

Marcos, R; Lopes, C; Malhao, F; Correia-Gomes, C; Fonseca, S; Lima, M; Gebhardt, R; Rocha, E

Published in:
Journal of Anatomy

DOI:
[10.1111/joa.12448](https://doi.org/10.1111/joa.12448)

First published: 01/01/2016

Document Version
Peer reviewed version

[Link to publication](#)

Citation for published version (APA):

Marcos, R., Lopes, C., Malhao, F., Correia-Gomes, C., Fonseca, S., Lima, M., ... Rocha, E. (2016). Stereological assessment of sexual dimorphism in the rat liver reveals differences in hepatocytes and Kupffer cells but not hepatic stellate cells. *Journal of Anatomy*, 228(6), 996 - 1005. <https://doi.org/10.1111/joa.12448>

General rights

Copyright and moral rights for the publications made accessible in the public portal are retained by the authors and/or other copyright owners and it is a condition of accessing publications that users recognise and abide by the legal requirements associated with these rights.

- Users may download and print one copy of any publication from the public portal for the purpose of private study or research.
- You may not further distribute the material or use it for any profit-making activity or commercial gain
- You may freely distribute the URL identifying the publication in the public portal ?

Take down policy

If you believe that this document breaches copyright please contact us providing details, and we will remove access to the work immediately and investigate your claim.

1 Stereological assessment of sexual dimorphism in the rat liver reveals differences in
2 hepatocytes and Kupffer cells but not hepatic stellate cells

3
4 Ricardo Marcos^{1,2}, Célia Lopes^{1,2}, Fernanda Malhão^{1,2}, Carla Correia-Gomes³, Sónia
5 Fonseca⁴, Margarida Lima⁴, Rolf Gebhardt⁵, Eduardo Rocha^{1,2}

6
7 ¹ Laboratory of Histology and Embryology, Department of Microscopy, ICBAS -
8 Institute of Biomedical Sciences Abel Salazar, U.Porto - University of Porto, Portugal

9 ² Histomorphology, Physiopathology and Applied Toxicology Group, CIIMAR -
10 Interdisciplinary Centre of Marine and Environmental Research, U.Porto, Portugal

11 ³ Scotland's Rural College, Epidemiology Research Unit- Future Farming Systems
12 Group. Inverness, United Kingdom.

13 ⁴ Laboratory of Cytometry, Department of Hematology, HSA – Hospital de Santo
14 António, CHP – Centro Hospitalar do Porto, UMIB – Unit for Multidisciplinary
15 Research in Biomedicine, ICBAS - Institute of Biomedical Sciences Abel Salazar,
16 U.Porto - University of Porto, Portugal.

17 ⁵ Institute of Biochemistry, Faculty of Medicine, University of Leipzig, Leipzig,
18 Germany.

19
20 Running title: Male versus female differences in the liver.

21
22 Keywords: Hepatic stellate cells, Kupffer cells, hepatocytes, liver, dimorphism,
23 stereology.

24
25 Corresponding author: Ricardo Marcos (DVM, MD, PhD)

26 Laboratory of Histology and Embryology
27 Institute of Biomedical Sciences Abel Salazar
28 Rua de Jorge Viterbo Ferreira no. 228,
29 4050-313 Porto, Portugal
30 Email: rmarcos@icbas.up.pt

31

32 **Abstract**

33 There is long-standing evidence that the male and female rat liver differ in enzyme
34 activity. More recently, differences in gene expression profiling have also been found to
35 exist; however, it is still unclear whether there is morphological expression of
36 male/female differences in the normal liver. Such differences could help to explain
37 features seen at the pathological level, such as the greater regenerative potential
38 generally attributed to the female liver. In this paper, hepatocytes (HEP), Kupffer cells
39 (KC) and hepatic stellate cells (HSC) of male and female rats were examined to
40 investigate hypothesized differences in number, volume and spatial co-localization of
41 these cell types. Immunohistochemistry and design-based stereology were used to
42 estimate total numbers, number per gram and mean cell volumes. The position of HSC
43 within lobules (periportal versus centrilobular) and their spatial vicinity to KC was also
44 assessed. In addition, flow cytometry was used to investigate the liver ploidy. In the
45 case of HEP and KC, differences in the measured cell parameters were observed
46 between male and female specimens; however, no such differences were detected for
47 HSC. Female samples contained a higher number of HEP per gram, with more
48 binucleate cells. The HEP nuclei were smaller in females, which was coincident with
49 more abundant diploid particles in these animals. In the case of KC, the female liver
50 also had a greater number per gram, with a lower percentage of KC in the vicinity of
51 HSC compared to males. In this study, we document hitherto unknown morphological
52 sexual dimorphism in the rat liver, namely in HEP and KC. These differences may
53 account for the higher regenerative potential of the female liver and lend weight to the
54 argument for considering the rat liver as a sexually dimorphic organ.

55

56 **Introduction**

57 Biological inequality is related to so-called gender or sexual dimorphism, in which
58 females have an increased resistance to premature ageing, nutrient deprivation, vascular
59 and heart diseases, brain disorders, as well as hepatic neoplasms and hepatitis C virus
60 infection (Li et al. 2012; Grebely et al. 2014). Evidence has mounted over the past thirty
61 years to demonstrate that the mammalian liver is responsive to steroid sex hormones.
62 These can modulate many functional features of the organ; apart from the differences in
63 cytochrome-P-450, diverse contents of glucose-6-phosphatase (Teutsch, 1984),
64 glutamine synthetase (Sirma et al. 1996) and lipogenic enzymes (Scheicher et al. 2015)
65 have been reported. Pathological features are also modulated by sex hormones,
66 illustrated by the fact that progression to cirrhosis in men can occur at a rate 10-times
67 faster than that seen in women (Poynard et al. 2001; Massard et al. 2006; Villa, 2008).
68 *In vitro* studies showed that oestrogens have antioxidant properties, reducing
69 proliferation and collagen synthesis in cultured hepatic stellate cells (HSC) (Yasuda et
70 al. 1999). There is no doubt that, at first sight, the microscopic morphology of the liver
71 appears similar in both sexes; however, it is unknown whether male and female HSC
72 differ in volume, number, surrounding cells or position within the liver lobules. Since
73 HSC are deeply influenced by the surrounding milieu (Kmieć, 2001), such differences
74 would explain, at least partially, the faster progression of collagen deposition in males.
75 The liver also exhibits sexual dimorphism in its capacity to regenerate. Unlike most
76 organs, the liver can increase its cell numbers after injury, restoring the lost mass to
77 obtain its optimal volume. Experimental studies in rats have shown a higher degree of
78 regeneration in females (Tsukamoto & Kojo 1990; Biondo-Simões et al. 2006;
79 Kitagawa et al. 2009) and the scarce clinical data in humans also points in the same
80 direction (*e.g.*, Imamura et al. 1999). Liver regeneration is of utmost importance in liver
81 transplantation, namely when “small for size” grafts are used. Among the many
82 proliferation factors, the “augmenter of liver regeneration” is an enigmatic protein
83 released by hepatocytes (HEP) that promotes liver growth (Gandhi, 2015). Recently, it
84 was shown that hepatocellular proliferation depends on the integrity of the Kupffer cells
85 (KC), since their depletion with gadolinium chloride significantly reduced the increase
86 in organ weight, as well as survival after small-for-size transplantation among a cohort
87 of rats (Yang et al. 2013). Still, the ratio of KC to HEP remains scarcely studied (Santos
88 et al. 2009), and it remains unknown if this ratio differs between the sexes. Intersexual

89 differences in HEP and KC could help to explain the increased risk of graft loss in
90 female-to-male liver transplants (Lai et al. 2011; Croome et al. 2014).

91 A potential mechanism behind the dimorphic liver regeneration is related to ploidy
92 differences, since diploid HEP are known to divide more rapidly than polyploid cells
93 after hepatectomy (Gupta, 2000). Cell ploidy is classically related to the cell volume
94 (Epstein, 1967), but male versus female differences in this parameter have never been
95 detailed by morphometry or stereology. Nevertheless, it would be interesting to relate
96 such data to DNA staining with propidium iodide and flow cytometry, which are well
97 recognized tools to evaluate ploidy, based on cell DNA content (Gupta, 2000).

98 In view of the state of the art, we hypothesized that there are structural differences in the
99 normal liver of males and females that could help explain differences in pathological
100 scenarios. To help elucidate the hypothesis, we combined design-based stereology and
101 flow cytometry to disclose sexual dimorphism in selected targets cells of the rat liver.
102 We first checked if significant differences existed in collagen in the lobules, the main
103 endpoint of HSC activity. Apart from evaluating the total number and number per gram,
104 we looked at the volume and intralobular position of these cells. Since it is recognized
105 that the first fibrogenic stimulus is modulated by KC, we not only estimated their total
106 number and number per gram but also quantified their vicinity to HSC. Moreover, we
107 also examined the numbers and percentage of binucleate hepatocytes (BnHEP), as well
108 as their cell and nuclear volume. The latter data enabled us to better evaluate, by a
109 morphological approach, if differences in ploidy existed across males and females.
110 These were later evaluated by a flow cytometry approach.

111

112 **Materials and Methods**

113 *Animals*

114 We used male and female Wistar rats (n = 5 per group) aged 2 months old, bought from
115 Charles-River Laboratories (Barcelona, Spain). All animals had been weaned at 20 days
116 and kept in standard conditions, receiving water and food ad-libitum in a controlled
117 environment [temperature of 25 °C and 12 hours alternated light-dark cycles, with light
118 period starting at 7.00 AM]. Males weighed 351 ± 17 g and females 216 ± 13 g. The
119 management of animals and procedures followed the European Union Directives
120 (1999/575/CE and 2010/63/UE) for the protection of animals used for scientific
121 purposes.

122

123 *Tissue Preparation*

124 Sampling was performed during the morning period (from 10 to 12 AM), to circumvent
125 oscillations in liver functions due to circadian rhythmicity (Davidson et al. 2004). In
126 females, daily vaginal cytologies were observed, in order to avoid collecting samples in
127 proestrous/oestrous days. Beforehand, animals were deeply anaesthetised with ketamine
128 plus xylazine and blood was collected from the heart and centrifuged to obtain serum
129 for assessing alanine and aspartate transaminase levels. Transcardiac perfusion was
130 performed for 15 minutes with an isosmotic solution, the liver was weighed and its
131 volume determined by the Scherle's method, as detailed elsewhere (Marcos et al. 2012).
132 A smooth fractionator sampling scheme was applied: half of the paraffin blocks were
133 used for thick sections (30 μ m thick) and exhaustively sectioned in a motorised
134 microtome, whilst the other half were used for thin sections (3 μ m thick) (Fig. 1). In
135 thick sections, we sampled five sections in every 30, which were immunostained
136 against: 1) glial fibrillary acidic protein for estimating the total number and number per
137 gram of HSC; 2) ED2 for estimating these parameters in KC; 3) E-cadherin, to
138 differentiate mononucleated from BnHEP, estimating their percentage, and assessing
139 the total number and number per gram of HEP; 4) glial fibrillary acidic protein and
140 glutamine synthetase [an established marker of centrilobular HEP (Gebhardt & Mecke
141 1983)], to evaluate the lobular distribution of HSC; 5) glial fibrillary acidic protein and
142 ED2 to study the vicinity between HSC and KC. As to the thin sections, these were used
143 for immunohistochemistry against glial fibrillary acidic protein, to determine the
144 relative volume of HSC, and for histochemical staining with Sirius red, to assess the
145 relative volume of fibrous tissue (Fig. 1).

146

147 ***Thick Sections***

148 *Immunohistochemistry*

149 The protocol used for thick sections has been previously described (Marcos et al. 2004;
150 2006). Briefly, antigen recovery was carried out in a microwave (four plus four minutes,
151 at 600 W) and a streptavidin-biotin protocol was used (Histostain Plus, Invitrogen,
152 Camarillo, California). For glial fibrillary acidic protein, we used 1:3000 rabbit
153 polyclonal antibody (Dako, Glostrup, Denmark), whereas for ED2 and E-cadherin we
154 used monoclonal mouse antibodies, from Serotec (United Kingdom) diluted at 1:100
155 and from Dako (clone NCH 38) diluted at 1:250, respectively. All slides were incubated
156 for four days at 4°C.

157 Slides for double immunohistochemistry were also placed in the microwave (this time
158 for three cycles of four minutes). After blocking endogenous biotin and peroxidase, the
159 first streptavidin-biotin protocol followed, with antibody against glial fibrillary acidic
160 protein (1:1500 dilution for four days at 4°C). Slides were developed for two minutes in
161 0.05% 3,3'-diaminobenzidine (Dako) in Tris-buffered saline with 0.03% H₂O₂ and
162 were then rinsed in tap-water and dipped in 50 mM glycine buffer (pH = 2.2) for five
163 minutes, to strip off the antibodies of the first immunoreaction. The second streptavidin-
164 biotin protocol followed, using 1:4000 rabbit polyclonal antibody against glutamine
165 synthetase (kindly gifted by Professor Rolf Gebhardt, University of Leipzig), for
166 another four days at 4°C. Slides were developed with aminoethylcarbazole (Dako) for
167 10 to 20 minutes (the final red colour was controlled by microscopic observation) and
168 slides were mounted in Aquatex (Dako). Regarding the double immunohistochemistry
169 to evaluate the vicinity of HSC and KC, the protocol was similar to the above described,
170 except for the second antibody (ED2 at 1:100 dilution).

171

172 *Stereological Analysis*

173 We used a stereology workstation detailed elsewhere (Marcos et al. 2004) with an
174 Olympus CAST-Grid software (version 1.5, Olympus). At the monitor, a final
175 magnification of 4750x allowed an easy and accurate recognition of all cells.
176 Throughout the disector height (20 µm), a software-generated counting frame was
177 superimposed with defined areas (1673 µm², 1267 µm² and 418 µm² for HSC, KC and
178 HEP, respectively). In the slides used for assessing the position of HSC within the
179 lobule, a systematic uniform random sampling was also used, but HSC were counted

180 only if fields were in the vicinity of the portal tracts or central venules (we settled these
181 areas as 5-6 HEP around these landmarks). For the double immunohistochemistry of
182 HSC and KC, the largest counting grid was used and a minimum of 100 HSC were
183 evaluated per animal (Fig. 2).

184 For counting cells, the nucleus was selected as the counting unit (in the case of BnHEP,
185 this was predetermined to be the first nucleus appearing in focus). Cells were counted
186 following the optical disector rules (Marcos et al. 2004; 2006). The potential bias from
187 lost caps was avoided by having upper and lower guard heights, which have previously
188 been validated for the rat liver (Marcos et al. 2012). The collapse in the z -direction was
189 also evaluated, by measuring the full section thickness with the microcator in every fifth
190 field (Dorph-Petersen et al. 2001).

191 The total number of HSC, KC and HEP in the whole liver was primarily estimated
192 according to the optical fractionator rules, meaning that the inverse of block, section,
193 area and height sampling fraction were multiplied by the number of cells counted in the
194 disectors (Marcos et al. 2012). Simultaneously, the number per gram was determined, as
195 this can aid when comparing values between animals with different liver weights. The
196 coefficient of error of the number of cells counted was estimated, using formulae
197 described elsewhere (Marcos et al. 2004).

198 Additionally, the number-weighted mean cell and nuclear volume of mononuclear and
199 BnHEP was estimated by the nucleator method (Gundersen, 1988; Marcos et al. 2012).
200 In this case, HEP were firstly sampled by the optical disector and their nucleolus
201 selected. Afterwards, the software generated two isotropic lines from the nucleolus and
202 the intersections between these lines and nuclear and cell borders were marked. The
203 average distance from the intersections to the nucleolus was used to estimate the
204 number-weighted mean cell and nuclear volume. In the case of HEP with two nucleoli
205 (or more), the measurements were performed for the two (or more) particles
206 (Gundersen, 1988).

207 Positive and negative controls (omission of first antibody and replacement by non-
208 immune serum) were included, both in thin and thick sections, and all slides were
209 blindly evaluated (*i.e.*, the observer was unaware of the sex of the animal), in order to
210 avoid eventual observer-related bias.

211

212

213

214 ***Thin Sections***

215 ***Immunohistochemistry***

216 A streptavidin–biotin protocol was also used (Histostain Plus) for glial fibrillary acidic
217 protein immunostaining. In this case, shorter incubation times were needed: the
218 antibody was diluted to 1:1200 and incubated overnight, whilst the blocking solution,
219 secondary antibody and streptavidin–peroxidase complex were all applied for 20
220 minutes; colour development in DAB was restricted to two minutes.

221

222 ***Histochemical Sirius red staining***

223 Thin sections were counterstained with celestial blue and Mayer’s haematoxylin, each
224 for five minutes; then, after washing in tap water, the Sirius red (Sigma, coloration
225 index 35782) dissolved in picric acid (1 mg/ml) was applied for one hour at room
226 temperature (Junqueira et al. 1978). After washing in acidified water (1% acetic acid),
227 sections were dehydrated, cleared and mounted.

228

229 ***Stereological analysis***

230 Five sections were randomly selected per animal and an average of 150 oil-immersion
231 fields were quantified per animal (fields were “selected” after systematic uniform
232 random sampling performed by the software). A test-system of points was
233 superimposed by the software in order to determine the relative volume of HSC in the
234 slides immunostained against glial fibrillary acidic protein (Fig. 3). The test-system
235 included 12 sparser points, used to quantify the reference space (whole liver) and 108
236 denser ones used for HSC. The relative volume of HSC was estimated as a ratio of the
237 two sets of points (Marcos et al. 2012). This parameter was multiplied by the liver
238 volume and divided by the total number of HSC in order to estimate the number-
239 weighted mean cell volume of HSC (Marcos et al. 2012).

240 The amount of collagen in Sirius red stained slides was also evaluated by a similar
241 strategy, but with 40x magnification lens (rendering a final magnification of 1600x at
242 the screen) and a scanner test system of 36 points (which was judged adequate to
243 estimate the relative volume of collagen). Point counting was used to determine the
244 relative volume of fibrous tissue (collagen I and III) in the liver, focusing on three
245 different locations: 1) Glisson’s capsule; 2) vascular (portal spaces and around central
246 veins); 3) intralobular (surrounding sinusoids).

247

248 *Flow cytometry*

249 In order to determine ploidy differences, liver pieces (≈ 0.7 g) frozen at -80°C were
250 gently thawed in phosphate buffered saline ($\text{pH} = 7.4$), and mechanically disaggregated
251 with tweezers. The homogenate was centrifuged at 750 G for five minutes, and the
252 supernatant decanted. The pellet was suspended in phosphate buffered saline and the
253 cell yield calculated in a haematology analyser (LH 780, Beckman Coulter, Brea,
254 California). Afterwards, the suspension was split into two parts: one for cytological
255 examination (cytospins) and the other for flow cytometry. For the latter, one 100 μl
256 aliquot of each sample (with an average of 3×10^6 cells/ μl) was stained using the Coulter
257 DNA-Prep Reagents Kit (Beckman Coulter), according to the manufacturer's
258 instructions. This was performed by sequentially dispensing and mixing 100 μl of the
259 lysing and permeabilising reagent (DNA Prep LPR), and 1 ml of the staining solution
260 containing 50 $\mu\text{g/ml}$ propidium iodide and 4 KU/ml bovine pancreas type III RNAase
261 (DNA Prep Stain) and finally, samples were incubated for 20 minutes in the dark. For
262 the flow cytometry analysis a Coulter EPICS-XL-MCL (Beckman Coulter) with a
263 488 nm argon ion laser was used. Sample acquisition was performed for a minimum of
264 30 minutes and a minimum of 20,000 events per sample were acquired. Rat
265 lymphocytes were employed as a control for diploid cells. Analysis was performed with
266 the MultiCycle software (Phoenix Flow Systems, San Diego), with modified
267 exponential debris function. The percentage of diploid, tetraploid and octaploid particles
268 was assessed.

269

270 *Statistical analysis*

271 The software SPSS 18 (IBM, Armonk, United States of America) was used. After
272 checking if the data followed a normal distribution with the Shapiro-Wilk's test, a
273 correlation analysis was conducted to detect linear correlations. Subsequent to assessing
274 the homogeneity of variances (Levene's test), the Student's t-test for unpaired samples
275 was used for comparing the means from males and females. In the case of liver weight,
276 relative volume of collagen and variables related with HSC (total number, number per
277 gram, number-weighted mean cell volume and lobular distribution), the non-parametric
278 equivalent, Mann-Whitney's U-test, was used for comparing medians from males and
279 females. Significance level was set at $p \leq 0.05$.

280

281 **Results**

282 Livers displayed a normal morphology, without noticeable differences across animals.
283 The livers of males were significantly heavier ($p = 0.02$) than those of females ($14.11 \pm$
284 2.9 g versus 9.75 ± 0.7 g, respectively). Likewise, male livers were significantly larger.
285 The liver-to-body weight ratio was 4.0 ± 0.7 % and 4.5 ± 0.6 % in males and females,
286 respectively. A very strong correlation was observed between liver and body weight ($r =$
287 0.8 ; $p = 0.01$). Hepatic transaminases values were within the reference ranges (14-80
288 IU/L for alanine and 40-383 for aspartate transaminase levels), presenting no significant
289 differences (42.0 ± 5.6 IU/L and 29.3 ± 10.9 IU/L for alanine and 98.8 ± 52.8 IU/L and
290 88.0 ± 42.2 IU/L for aspartate transaminase in males and females, respectively).

291

292 *Thick sections*

293 An average of 509 and 273 disectors were analysed for male and female rats,
294 respectively. The total number of HSC was significantly higher in males than in females
295 ($p = 0.016$), but their number per gram was similar (Table 1). By way of contrast, the
296 total number of HEP was similar in males and females, although the latter had a
297 significantly higher number per gram ($p = 0.016$). The same was seen for the BnHEP
298 and KC: where the number per gram was significantly higher in females ($p = 0.016$), but
299 the total number was similar in both sexes. The proportion of BnHEP, was $24.8 \pm 4.2\%$
300 for males and $33.8 \pm 4.7\%$ for females indicating no significant difference. It is
301 noteworthy that the coefficient of error of the number estimations of HSC, HEP and KC
302 was low, being between 0.039 and 0.060. This means that the methodological
303 variability contributed much less to the total variance than the biological component
304 (the latter was responsible for 80-93% of the total variance).

305 A very strong correlation was observed between the total number of HSC and liver
306 weight ($r = 0.85$, $p = 0.004$). In addition, the number per gram of HEP was also
307 correlated with that of KC and with the number per gram of BnHEP ($r = 0.94$, $p < 0.001$
308 and $r = 0.75$, $p = 0.02$, respectively). The relative volume of intralobular collagen was
309 correlated only with the total number of HEP ($r = 0.74$, $p = 0.037$) — this correlation
310 was mainly with mononucleated HEP, since no correlation existed with the number of
311 BnHEP. As to the percentage of BnHEP, it was negatively correlated with the body
312 weight ($r = -0.81$, $p = 0.015$) and total number of HEP ($r = -0.76$, $p = 0.028$).

313 The number-weighted mean cell and nuclear volume of HEP were also evaluated; on
314 average, 107 HEP per animal were assessed for these purposes (Table 2). Male versus

315 female differences existed for mononucleated HEP ($p = 0.002$), but not for BnHEP.
316 Mononucleated cells were 21% to 34% smaller than BnHEP ($p < 0.001$). With regard to
317 the number-weighted mean nuclear volume, significant male/female differences existed
318 for mononucleated HEP ($p = 0.029$). The histogram of the number-weighted mean
319 nuclear volume revealed small differences: young females exhibited a slightly skewed
320 pattern (Pearson's skewness = 1.0; kurtosis = 3.38) compared to males (Pearson's
321 skewness = 0.34; kurtosis = 0.51) (Fig. 4). Considering that the histogram featured two
322 modes, observed in data from both females and males, we computed this as two
323 distributions (one for diploid cells and the other for tetraploid cells). The first mode was
324 considered the mean of the diploid cells and the second the mean of the tetraploid cells.
325 The standard deviation for each group was calculated based on the means. In this way,
326 we estimated the number-weighted mean nuclear volume of the diploid nuclei as $225 \pm$
327 $36 \mu\text{m}^3$, whereas the tetraploid nuclei had a mean volume of $447 \pm 52 \mu\text{m}^3$. The
328 number-weighted mean nuclear volumes of mononucleated HEP and BnHEP were not
329 significantly correlated with their respective cell volumes ($p = 0.085$ and 0.072 ,
330 respectively). In BnHEP, the two nuclei presented volumes of the same order of
331 magnitude, but the coefficient of variance between nuclei varied up to 14%. The nuclear
332 to cytoplasm ratio was between 9.2% and 11.9% and no differences existed between
333 mononucleated and BnHEP.

334 For the distribution of HSC in liver lobules, we evaluated an average of 303 HSC per
335 animal and cells were significantly more abundant in centrilobular regions ($56.5 \pm$
336 4.5%) than in periportal locations ($43.3 \pm 4.3\%$) ($p = 0.001$). The distribution of cells
337 was similar in males and females and no staining intensity differences could be detected
338 between these locations. As to cells neighbouring HSC, we should stress that the thick
339 sections, encompassing all KC and HSC cell processes, allowed easy recognition of cell
340 juxtapositions (Fig. 2). On average, we evaluated 188 HSC per animal, noting that 41.6
341 $\pm 6.7\%$ were physically positioned next to KC in males. In females a lower number of
342 HSC ($26 \pm 7.4\%$) had KC for neighbours; the difference in the position of these two
343 cells was statistically significant ($p = 0.001$).

344

345 *Thin sections*

346 An average of 216 fields was screened per animal. In males, the intralobular collagen
347 corresponded to 56% of the total collagen, whereas 20% and 14% were located in portal
348 tracts and around central venules respectively and only 10% was found in the Glisson's

349 capsule. A similar scenario existed in females: 46 % was intralobular, 42% around
350 vessels (respectively, 28% and 14% in a portal and central location) and 12% in the
351 capsule. No significant differences existed in these proportions between males and
352 females. As to the collagen content in the liver, no differences existed between males
353 ($2.05 \pm 0.2\%$) and females ($1.95 \pm 0.3\%$).

354 In thin paraffin sections we also evaluated the relative volume of HSC immunostained
355 by glial fibrillary acidic protein (Fig. 3). No statistical differences existed for this
356 parameter across the sexes (Table 1). Regarding the number-weighted mean cell volume
357 of HSC, no statistical differences were noted: male and female HSC had $619 \pm 128 \mu\text{m}^3$
358 and $786 \pm 192 \mu\text{m}^3$, respectively.

359

360 *Flow cytometry*

361 The mechanical dissociation of the liver rendered a mixture of particles, mostly formed
362 by HEP nuclei (easily identified by their large size and presence of nucleoli) and well
363 preserved HEP (both mononucleated and BnHEP), in variable proportions. Owing to the
364 mechanical dispersion of the liver cells and to the washing procedure, followed by slow
365 speed centrifugation, non-hepatocytes were present in low numbers (an average of less
366 than 5% of the nuclei, as verified by light microscopy, in the cytospin smears).

367 The flow cytometry analysis showed that the percentage of diploid particles (i.e., naked
368 nuclei with 2N mixed with cells with 2N) tended to be more abundant in females (Table
369 3): significant differences existed between males and females ($p = 0.02$). No octaploid
370 particles were observed.

371

372 **Discussion**

373 In this paper, we document, for the first time, the existence of linear correlations across
374 liver cells. Apart from the strong correlation between the liver weight and the total
375 number of HSC, these were also correlated with HEP; furthermore, correlations were
376 established with BnHEP and KC. This emphasizes the complex functional interplay that
377 takes place in the liver, which will be discussed below, cell by cell.

378

379 *Hepatic stellate cells*

380 Since liver fibrosis differs across sex in humans and rats, it could be hypothesized that
381 baseline microanatomical differences in HSC exist in the normal organ. However, this
382 was not backed by our data, as no quantitative differences were observed.

383 With regard to collagen deposition, a well recognized end-product of HSC (Friedman,
384 2008), no sexual differences exist and this is in accordance with previous studies that
385 estimated collagen via hydroxyproline content (*e.g.*, Shimizu et al. 1999). Our
386 estimation of the relative volume of collagen and its distribution in the liver are also in
387 accordance with previous studies (Harkness & Harkness 1954; Gascon-Barré et al.
388 1989). The synthesis of extracellular matrix and collagen in normal liver is ascribed to
389 various cell types besides HSC, including HEP and liver sinusoidal endothelial cells
390 (Friedman, 2008), but surprisingly, of the three cell types examined here, we found a
391 correlation only with HEP. This suggests that these cells may be the most relevant for
392 collagen production in a normal setting, contrasting with cirrhotic livers, in which HSC
393 have a leading role (Gressner & Weiskirchen 2006).

394 The mean cellular volume of HSC has, to the best of our knowledge, never been
395 reported. In this study, we opted for an indirect approach to estimate the number-
396 weighted mean cell volume, because local estimators (for instance the nucleator) would
397 be extremely difficult to implement. HSC have cellular extensions expanding in various
398 directions (Oikawa et al. 2002) that would be in and out of focus in thick sections. It
399 should be noted that our estimation ($\approx 700 \mu\text{m}^3$ in males and females) is satisfactory for
400 practical purposes but represents a slight underestimation, because we highlighted the
401 cytoskeleton and not the cell borders. Regarding volume estimation and HSC, the single
402 study that estimated their relative volume obtained values of $0.4 \pm 0.1\%$ (Martin et al.
403 1992a), which is comparable to our figure ($0.3 \pm 0.1\%$).

404 The lobulation of HSC has never been studied by stereology but has been a
405 controversial topic. Herein, we reported a pericentral predominance in both males and

406 females, but Wake (1980) and Geerts et al. (1991) — using vitamin A autofluorescence
407 and immunohistochemistry against desmin, respectively — reported a periportal
408 predominance. Nevertheless, Higashi & Senoo (2003) and Senoo et al. (2007) used
409 similar methods but found no lobular differences. The fact that we used antigen retrieval
410 and long incubation times in paraffin sections (in contrast with cryostat sections of most
411 studies) probably accounts for the differences. Moreover, a stereological strategy in
412 thick sections should be more reliable for quantifying lobular heterogeneity, since thin
413 sections viewed at low magnification naturally tend to a bias towards periportal areas,
414 which are far more cellular (Teutsch et al. 1999).

415

416 *Hepatocytes*

417 Sexual differences in HEP have never been evaluated by quantitative morphology, as
418 far as we are aware. Regarding their total number, we did not observe significant
419 male/female differences — even if they could be expected due to the geometric scaling
420 related to a larger liver and body size of males. Surprisingly, sexual dimorphism was
421 evident when assessing number of HEP per gram, the so-called hepatocellularity. This
422 parameter is important, not only because it allows a straightforward comparison
423 between studies, but also because it is widely used when *in vivo* hepatic clearance needs
424 to be predicted (Barter et al. 2007). Using different methodologies, hepatocellularity in
425 the male rat has ranged from 85×10^6 HEP per gram (Carlile et al. 1997) to almost
426 double that figure at 163×10^6 HEP per gram (Smith et al. 2008); in humans, the value of
427 120×10^6 HEP per gram has been predicted from the study of liver microsomes (Hirota et
428 al. 2001). Sexual differences have been rarely considered, but Atchley et al. (2000)
429 proposed their existence in mice (after puberty), with females having significantly more
430 and smaller HEP than males; overall, this is in accordance with our data. The higher
431 hepatocellularity in females may be explained by effects of oestrogens, since, at least *in*
432 *vitro*, ethinylestradiol has induced a 7-fold increase in HEP proliferation, with DNA
433 synthesis, but without cytotoxicity or induction of cytochrome-P-450 (Vickers and
434 Lucier 1996). A pioneer study by Fisher et al. (1984) also showed that the livers of
435 female rats receiving multiple injections of estradiol were 27% heavier and had an
436 increase of total DNA.

437 We highlighted a negative correlation between BnHEP percentage and body and liver
438 weight. A negative correlation between binuclearity, nuclear ploidy and body weight

439 seems to be a feature of mammals, including rats (Vinogradov et al. 2001). It has been
440 known for more than sixty years (St Aubin & Bucher 1952) that the percentage of
441 BnHEP decreases whilst the total number of HEP increases during normal rat growth
442 and in partial hepatectomy. This phenomenon is also suggested by our data, by the
443 negative correlation between the percentage of BnHEP and the total number of HEP.
444 Even if no sexual differences existed in the percentage of BnHEP, we observed
445 significant differences in their number per gram. This could be related to insulin, since
446 *in vitro* studies have demonstrated that epidermal growth factor and insulin induced a
447 high rate of BnHEP, similar to that normally observed in the liver of growing rats
448 (Mossin et al. 1994). More recently, it was reported that rats with low insulin levels had
449 less formation of BnHEP compared to animals injected with the hormone (Celton-
450 Morizur & Desdouets 2010). Interestingly, differences in insulin also appear to exist in
451 normal rats with higher levels in females (Da Costa et al. 2004; Vital et al. 2006).
452 Oestrogens may also play a role here, since oophorectomised rats have significantly
453 lower insulin levels that can be restored with estradiol administration (Ahmadi & Oryan
454 2008). The functional significance of sexual dimorphism in the number per gram of
455 HEP and BnHEP is still unknown, but it may underlie the larger functional reserve and
456 the higher regenerative potential reported for the female liver (Shimizu et al. 2007).
457 Another interesting finding of our study relates to the volume of HEP. It is often
458 assumed that BnHEP are twice the size of mononucleated HEP (*e.g.*, Celton-Morizur &
459 Desdouets 2010; Crawford & Burt 2012). Since a twofold increase in volume
460 corresponds to only a 1.4-fold increase in surface area, this would result in less efficient
461 transport in BnHEP (Pandit et al. 2013). The twofold assumption has been substantiated
462 by classical studies which dissociated HEP mechanically (Epstein, 1967, Martin et al.
463 1992b). It should be noted that isolated HEP tend to enlarge, because they do not have
464 compressive forces of adjacent cells and they often appear flattened (and further
465 enlarged) bellow the coverslip (St Aubin & Bucher 1952). Our data strongly contradicts
466 a twofold proportionality because the number-weighted mean cell volume of BnHEP is
467 only 25% to 37% larger than that of mononucleated HEP and no correlation existed
468 between the number-weighted mean cell volume of these cells. In fact, the use of
469 different meshes to sort HEP after isolation has already showed that cell size is not
470 correlated with binuclearity or ploidy (Gandillet et al. 2003).
471 It should be emphasized that the number-weighted mean cell volume of HEP is an
472 important parameter in research, being considered the best predictor of liver cancer in

473 rodents (Hall et al. 2012). Overall, our data on the volume of HEP is coincident with
474 general figures reported [5000 to 6000 μm^3 (McCuskey, 2006, Grisham, 2009)] and
475 closely resembles those of Jack et al. (1990), who also used stereological methods.

476

477 *Kupffer cells*

478 To the best of our knowledge, this is the first report of sexual dimorphism in the number
479 per gram of KC. Notably it has been shown that female rats as well as mice have $\approx 50\%$
480 more macrophages than males, both in their pleural and peritoneal cavities, with more
481 toll-like receptors and more efficiency in phagocytosis (Scotland et al. 2011). Even if
482 new numerical differences were disclosed herein, it has been known for a long time that
483 KC are influenced by oestrogen: peaks of phagocytosis and proliferation have been
484 correlated with elevated oestrogen in the oestrous cycle of mice and rats (Nicol &
485 Veron-Roberts 1965; Vickers and Lucier 1996).

486 The HSC-KC vicinity should favour the crosstalk and paracrine/juxtacrine stimulation
487 among these cells, which is nowadays viewed as reciprocal (Tacke and Zimmermann
488 2014). Since liver sinusoids have fenestrae it is easy for intrasinusoidal KC to contact
489 directly with perisinusoidal HSC. The relationship between these cells has a long
490 history; it has been known for more than 25 years that the conditioned medium of KC is
491 able to stimulate collagen synthesis and activation of HSC (Friedman & Arthur 1989),
492 whereas HSC-derived molecules promote the differentiation of a more pro-
493 inflammatory and pro-fibrotic phenotype of KC (Chang et al. 2013). Because sexual
494 differences exist in the constellation of HSC-KC — *viz.* $41.6 \pm 6.7\%$ and $26 \pm 7.4\%$ in
495 males and females, respectively — it could be hypothesized that a less pro-
496 inflammatory KC phenotype could be present in the female rat liver.

497 In conclusion, we have demonstrated that HEP and KC, but not HSC, have significant
498 sexual dimorphism. This may be due to oestrogens acting in receptors α , which
499 functionally exist in HEP and KC but not in HSC (Shimizu et al. 2007). In view of the
500 fact that mechanisms underlying clinically sexual dimorphism are largely unknown
501 (Yokoyama et al. 2007; Li et al. 2012), this study adds substantial understanding by
502 showing that primal morphological quantitative differences do exist in the rat liver. This
503 should be taken into account when planning studies and interpreting sexual-differences
504 in liver regeneration, inflammatory and fibrotic conditions. In addition, it would be
505 particularly interesting to investigate whether our findings in rats also apply to humans.

506

507 **Acknowledgments**

508 This work was financially supported by FEDER funds through the Competitiveness and
509 Trade Expansion Program (COMPETE) and by national funds, Fundação para a Ciência
510 e Tecnologia (FCT) via a doctoral grant (SFRH/BD/38958/2007). We are deeply
511 grateful to Madelaine Henry for English language editing.

512

513 **Conflict of interest**

514 The authors declare that they do not have any conflict of interest.

515

516 **References:**

517 **Ahmadi R, Oryan Sh** (2008) Effects of ovariectomy or orchidectomy and estradiol
518 valerate or testosterone enanthate replacement on serum insulin in rats. **Pak J Biol Sci**
519 **15**, 306-308.

520 **Atchley WR, Wei R, Crenshaw P** (2000) Cellular consequences in the brain and liver
521 of age-specific selection for rate of development in mice *Genetics* **155**, 1347-1357.

522 **Barter ZE, Bayliss MK, Beaune PH, et al.** (2007) Scaling factors for the
523 extrapolation of in vivo metabolic drug clearance from in vitro data: researching a
524 consensus on values of human microsomal protein and hepatocellularity per gram of
525 liver *Curr Drug Metab* **8**, 33-45.

526 **Biondo-Simões ML, Matias JE, Montibeller GR, Siqueira LC, Nunes E, Grassi CA**
527 (2006) Effect of aging on liver regeneration in rats. *Acta Cir Bras* **21**, 197-202.

528 **Carlile DJ, Zomorodi K, Houston JB** (1997) Scaling factors to relate drug metabolic
529 clearance in hepatic microsomes, isolated hepatocytes, and the intact liver: studies with
530 induced livers involving diazepam *Drug Metab Dispos* **25**, 903-911.

531 **Celton-Morizur S, Desdouets C** (2010) Polyploidization of liver cells. *Adv Exp Med*
532 *Biol* **676**, 123-135.

533 **Chang J, Hisamatsu T, Shimamura K, et al.** (2013) Activated hepatic stellate cells
534 mediate the differentiation of macrophages. *Hepatol Res* **43**, 658-669.

535 **Crawford JM, Burt AD** (2012) Anatomy, pathophysiology and basic mechanisms of
536 disease. In: *MacSween's Pathology of the liver*, 6th edition (eds Burt A, Portmann B,
537 Ferrell L), pp. 1-74. Edinburgh: Churchill Livingstone.

538 **Croome KP, Segal D, Hernandez-Alejandro R, Adams PC, Thomson A, Chandok**
539 **N** (2014) Female donor to male recipient gender discordance results in inferior graft

540 survival: a prospective study of 1,042 liver transplants. *J Hepatobiliary Pancreat Sci* **21**,
541 269-274.

542 **Lopes Da Costa C, Sampaio de Freitas M, Sanchez Moura A** (2004) Insulin
543 secretion and GLUT-2 expression in undernourished neonate rats. *J Nutr Biochem* **15**,
544 236-241.

545 **Davidson AJ, Castañón-Cervantes O, Stephan FK** (2004) Daily oscillations in liver
546 function: diurnal vs circadian rhythmicity. *Liver Int* **24**, 179-86.

547 **Dijkstra CD, Döpp EA, Joling P, Kraal G** (1985) The heterogeneity of mononuclear
548 phagocytes in lymphoid organs: distinct macrophage subpopulations in the rat
549 recognized by monoclonal antibodies ED1, ED2 and ED3. *Immunology* **54**, 589-599.

550 **Dorph-Petersen KA, Nyengaard JR, Gundersen HJG** (2001) Tissue shrinkage and
551 unbiased stereological estimation of particle number and size. *J Microsc* **204**, 232-246.

552 **Epstein CJ** (1967) Cell size, nuclear content, and the development of polyploidy in the
553 Mammalian liver. *Proc Natl Acad Sci USA* **57**, 327-334.

554 **Fisher B, Gunduz N, Saffer EA, Zheng S** (1984) Relation of estrogen and its receptor
555 to rat liver growth and regulation. *Cancer Res* **44**, 2410-2415.

556 **Friedman SL** (2008) Hepatic stellate cells: protean, multifunctional, and enigmatic
557 cells of the liver. *Physiol Rev* **88**, 125-172.

558 **Friedman SL, Arthur MJ** (1989) Activation of cultured rat hepatic lipocytes by
559 Kupffer cell conditioned medium. Direct enhancement of matrix synthesis and
560 stimulation of cell proliferation via induction of platelet-derived growth factor
561 receptors. *J Clin Invest* **86**, 1780-1785.

562 **Gandhi CR**. Augmenter of liver regeneration. *Fibrogenesis Tissue Repair* 2012;5:10.

563 **Gandillet A, Alexandre E, Holl V, et al.** (2003) Hepatocyte ploidy in the normal rat.
564 *Comp Biochem Physiol A Mol Integr Physiol* **134**, 665-673.

565 **Gascon-Barré M, Huet PM, Belgiorno J, Plourde V, Coulombe PA** (1989)
566 Estimation of collagen content of liver specimens. Variation among animals and among
567 hepatic lobes in cirrhotic rats. *J Histochem Cytochem* **37**, 377-381.

568 **Gebhardt R, Mecke D** (1983) Heterogeneous distribution of glutamine synthetase
569 among rat liver parenchymal cells in situ and in primary culture. *EMBO J* **2**, 567-570.

570 **Geerts A, Lazou JM, De Bleser P, Wisse E** (1991) Tissue distribution, quantitation
571 and proliferation kinetics of fat-storing cells in carbon tetrachloride-injured rat liver.
572 *Hepatology* **13**, 1193-1202.

573 **Grebely J, Page K, Sacks-Davis R, et al.** (2014) The effects of female sex, viral
574 genotype, and IL28 genotype on spontaneous clearance of acute hepatitis C virus
575 infection. *Hepatology* **59**, 109-120.

576 **Gressner AM, Weiskirchen R** (2006) Modern pathogenetic concepts of liver fibrosis
577 suggest stellate cells and TGF-beta as major players and therapeutic targets. *J Cell Mol*
578 *Med* **10**, 76-99.

579 **Grisham JW** (2009) Organizational principles of the liver. In: *The liver: biology and*
580 *pathobiology*, 5th edition (eds Arias IM, Alter HJ, Boyer JL, Cohen DE, Fausto N,
581 Shafritz DA, Wolkoff AW), pp. 3-15. New York: John Wiley & Sons Ltd.

582 **Gundersen HJ** (1988) The nucleator. *J Microsc* **151**, 3-21.

583 **Gupta S** (2000) Hepatic polyploidy and liver growth control. *Semin Cancer Biol* **10**,
584 161-171.

585 **Hall AP, Elcombe CR, Foster JR** (2012) Liver hypertrophy: a review of adaptative
586 (adverse and non-adverse) changes — conclusions from the 3rd international ESTP
587 expert workshop. *Toxicol Pathol* **40**, 971-994.

588 **Harkness ML, Harkness RD** (1954) Further observations on collagen in regenerating
589 liver of the rat. *J Physiol* **123**, 482-491.

590 **Higashi N, Senoo H** (2003) Distribution of vitamin A-storing lipid droplets in hepatic
591 stellate cells in liver lobules - a comparative study. *Anat Rec A Discov Mol Cell Evol*
592 *Biol* **271**, 240-248.

593 **Hirota N, Ito K, Iwatsubo T, et al.** (2001) In vitro/in vivo scaling of alprazolam
594 metabolism by CYP3A4 and CYP3A5 in humans. *Biopharm Drug Dispos* **22**, 53-71.

595 **Imamura H, Shimada R, Kubota M, et al.** (1999) Preoperative portal vein
596 embolization: an audit of 84 patients. *Hepatology* **29**, 1099-1105.

597 **Jack EM, Bentley P, Bieri F, et al.** (1990) Increase in hepatocyte and nuclear volume
598 and decrease in the population of binucleated cells in preneoplastic foci of rat liver: a
599 stereological study using the nucleator method. *Hepatology* **11**, 286-297.

600 **Junqueira LC, Cossermelli W, Brentani R** (1978) Differential staining of collagens
601 type I, II and III by Sirius Red and polarization microscopy. *Arch Histol Jap* **41**, 267-
602 274.

603 **Kitagawa T, Yokoyama Y, Kokuryo T, et al.** (2009) Estrogen promotes hepatic
604 regeneration via activating serotonin signal. *Shock* **31**, 615-620.

605 **Kmieć Z** (2001) Cooperation of liver cells in health and disease. *Adv Anat Embryol Cell*
606 *Biol* **161**, 1-151.

607 **Lai JC, Feng S, Roberts JP, Terrault NA** (2011) Gender differences in liver donor
608 quality are predictive of graft loss. *Am J Transplant* **11**, 296-302.

609 **Li Z, Tuteja G, Schug J, Kaestner KH** (2012) Foxa1 and Foxa2 are essential for
610 sexual dimorphism in liver cancer. *Cell* **148**, 72-83.

611 **Marcos R, Monteiro RA, Rocha E** (2004) Estimation of the number of stellate cells in
612 a liver with the smooth fractionator. *J Microsc* **215**, 174-182.

613 **Marcos R, Monteiro RAF, Rocha E** (2006) Design-based stereological estimation of
614 hepatocyte number, by combining the smooth optical fractionator and
615 immunocytochemistry with anticarcinoembryonic antigen polyclonal antibodies. *Liver*
616 *Int* **26**, 116-124.

617 **Marcos R, Monteiro RAF, Rocha E** (2012) The use of design based stereology to
618 evaluate volumes and numbers in the liver: a review with practical guidelines. *J Anat*
619 **220**, 303-317.

620 **Martin G, Sewell RB, Yeomans ND, Smallwood RA** (1992) Ageing has no effect on
621 the volume density of hepatocytes, reticulo-endothelial cells or the extracellular space in
622 livers of female Sprague-Dawley rats. *Clin Exp Pharmacol Physiol* **19**, 537-539.

623 **Martin NC, McCullough CT, Bush PG, Sharp L, Hall AC, Harrison DJ** (1992)
624 Functional analysis of mouse hepatocytes differing in DNA content: volume, receptor
625 expression and effect of INN γ . *J Cell Physiol* **191**, 138-144.

626 **Massard J, Ratziu V, Thabut D, et al.** (2006) Natural history and predictors of disease
627 severity in chronic hepatitis C. *J Hepatol* **44**, S19-24.

628 **McCuskey RS** (2006) Anatomy of the liver. In: *Zakim and Boyer's hepatology. A*
629 *textbook of liver disease*, 5th edition (eds Boyer TD, Wright TL, Manns MP), pp. 3-21.
630 Philadelphia: Saunders.

631 **Mossin L, Blankson H, Huitfeldt H, Seglen PO** (1994) Ploidy-dependent growth and
632 binucleation in cultured rat hepatocytes. *Exp Cell Res* **214**, 551-560.

633 **Nicol T, Veron-Roberts B** (1965) The influence of the estrus cycle, pregnancy and
634 ovariectomy on RES Activity. *J Reticuloendothel Soc* **60**, 15-29.

635 **Oikawa H, Masuda T, Kamaguchi J, Sato S** (2002) Three-dimensional examination
636 of hepatic stellate cells in rat liver and response to endothelin-1 using confocal laser
637 scanning microscopy. *J Gastroenterol Hepatol* **17**, 861-872.

638 **Pandit SK, Westendorp B, Bruin A.** Physiological significance of polyploidization in
639 mammalian cells. *Trends Cell Biol* 2013;23:556-566.

640 **Poynard T, Ratziu V, Charlotte F, Goodman Z, McHutchison J, Albrecht J** (2001)
641 Rates and risk factors of liver fibrosis progression in patients with chronic hepatitis C. *J*
642 *Hepatol* **34**, 730-739.

643 **Santos M, Marcos R, Santos N, Malhão F, Monteiro RAF, Rocha E** (2009) An
644 unbiased stereological study on subpopulations of rat liver macrophages and on their
645 numerical relation with the hepatocytes and stellate cells. *J Anat* **214**, 744-751.

646 **Scheicher J, Tokarski C, Marbach E, et al.** (2015) Zonation of hepatic fatty acid
647 metabolism - The diversity of its regulation and the benefit of modeling. *Biochim*
648 *Biophys Acta* **1851**, 641-656.

649 **Scotland RS, Stables MJ, Madalli S, Watson P, Gilroy DW** (2011) Sex differences in
650 resident immune cell phenotype underlie more efficient acute inflammatory responses in
651 female mice. *Blood* **118**, 5918-5927.

652 **Senoo H, Kojima N, Sato M** (2007) Vitamin A-storing cells (stellate cells). *Vitam*
653 *Hormon* **75**, 131-159.

654 **Shimizu I, Mizobuchi Y, Yasuda M, et al.** (1999) Inhibitory effect of oestradiol on
655 activation of rat hepatic stellate cells in vivo and in vitro. *Gut* **44**, 127-136.

656 **Shimizu I, Kohno N, Tamaki K, et al.** (2007) Female Hepatology: favorable role of
657 estrogen in chronic liver disease with hepatitis B virus infection. *World J Gastroenterol*
658 **13**, 4295-4305.

659 **Sirma H, Williams GM, Gebhardt R** (1996) Strain- and sex-specific variations in
660 hepatic glutamine synthetase activity and distribution in rats and mice. *Liver* **16**, 166-
661 173.

662 **Smith R, Jones RD, Ballard PG, Griffiths HH** (2008) Determination of microsome
663 and hepatocyte scaling factors for in vitro/in vivo extrapolation in the rat and dog.
664 *Xenobiotica* **38**, 1386-1398.

665 **St Aubin PM, Bucher NL** (1952) A study of binucleate cell counts in resting and
666 regenerating rat liver employing a mechanical method for the separation of liver cells.
667 *Anat Rec* **112**, 797-809.

668 **Tacke F, Zimmermann HW** (2014) Macrophage heterogeneity in liver injury and
669 fibrosis. *J Hepatol* **60**, 1090-1096.

670 **Teutsch HF** (1984) Sex-specific regionality of liver metabolism during starvation; with
671 special reference to the heterogeneity of the lobular periphery. *Histochemistry* **81**, 87-
672 92.

673 **Teutsch HF, Schuerfeld D, Groezinger E** (1999) Three-dimensional reconstruction of
674 parenchymal units in the liver of the rat. *Hepatology* **29**, 494-505.

675 **Tsukamoto I, Kojo S** (1990) The sex difference in the regulation of liver regeneration
676 after partial hepatectomy in the rat. *Biochim Biophys Acta* **1033**, 287-290.

677 **Vickers AE, Lucier GW** (1996) Estrogen receptor levels and occupancy in hepatic
678 sinusoidal endothelial and Kupffer cells are enhanced by initiation with
679 diethylnitrosamine and promotion with 17 alpha-ethinylestradiol in rats. *Carcinogenesis*
680 **17**, 1235-1242.

681 **Villa E** (2008) Role of estrogen in liver cancer. *Womens Health* **4**, 41-50.

682 **Vinogradov AE, Anatskaya OV, Kudryavtsev BN** (2001) Relationship of hepatocyte
683 ploidy levels with body size and growth rate in mammals. *Genome* **44**, 350-360.

684 **Vital P, Larrieta E, Hiriart M** (2006) Sexual dimorphism in insulin sensitivity and
685 susceptibility to develop diabetes in rats. *J Endocrinol* **190**, 425-432.

686 **Wake K** (1980) Perisinusoidal stellate cells (fat-storing cells, interstitial cells,
687 lipocytes), their related structure in and around the liver sinusoids, and vitamin A-
688 storing cells in extrahepatic organs. *Int Rev Cytol* **66**, 303-353.

689 **Yang K, Du C, Cheng Y, Li Y, Gong J, Liu Z** (2013) Augmenter of liver regeneration
690 promotes hepatic regeneration depending on the integrity of Kupffer cell in rat small-
691 for-size liver transplantation. *J Surg Res* **183**, 922-928.

692 **Yasuda M, Shimizu I, Shiba M, Ito S** (1999) Suppressive effects of estradiol on
693 Dimethylnitrosamine-induced fibrosis of the liver in rats. *Hepatology* **29**, 719-727.

694 **Yokoyama Y, Nagino M, Nimura Y** (2007) Which gender is better positioned in the
695 process of liver surgery? Male or female? *Surg Today* **37**, 823-830.

696

697 **Figure 1:** Overview of the methods used in this study in thin and thick liver sections
698 and in frozen pieces.

699






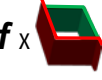
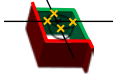
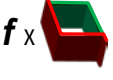


700 **Figure 2:** Thin liver section immune-stained against glial fibrillary acidic protein for
701 detecting hepatic stellate cells (HSC). The relative volume of HSC was estimated by
702 counting points falling within HSC and within the reference space (whole liver). In
703 order to avoid counting an excessive number of points, two different point densities
704 were used: the sparser points (in yellow) quantified the whole liver. Bar = 4 μm .

705

706 **Figure 3:** Thick liver section immune-stained against glial fibrillary acidic protein and
707 ED2 for detecting hepatic stellate cells (HSC, black arrows) and Kupffer cells (KC,
708 open arrows), respectively. Cells were counted if their nucleus was in focus below 4 μm
709 and above or equal to 24 μm in the z-axis (section depth), if they were inside the
710 inclusion (green) lines, or not touching the exclusion (red) lines. Bar = 6 μm .

711

712 **Figure 4:** Histogram of the number weighted mean nuclear volume of hepatocytes in
713 males (yellow) and female (blue). The volume of diploid nuclei was estimated to be 225
714 $\pm 36 \mu\text{m}^3$, whereas that of tetraploid nuclei was $447 \pm 52 \mu\text{m}^3$.

	Thick sections 						Thin sections 		Pieces 
Stain/Marker	GFAP-GS	GFAP	E-cadherine	E-cadherine	ED2	GFAP-ED2	Sirius red	GFAP	PI
Method		f_X 	f_X 		f_X 		++++ ++++ ++++	++++ ++++ ++++	
Assessment	Distribution of HSC	N of HSC	N of HEP	\bar{V}_N cell and HEP nuclei	N of KC	Colocalization HSC and KC	V_V collagen	V_V of HSC	ploidy

HEP: hepatocytes; HSC: hepatic stellate cells; KC: Kupffer cells; N: total number; V_V : relative volume, \bar{V}_N number weighted mean cell volume.

